TOTAL INTERNAL REFLECTION/FLUORESCENCE PHOTOBLEACHING RECOVERY STUDY OF SERUM ALBUMIN ADSORPTION DYNAMICS

THOMAS P. BURGHARDT AND DANIEL AXELROD, *Biophysics Research Division, and Department of Physics, University of Michigan, Ann Arbor, Michigan 48109 U.S.A.*

ABSTRACT The total internal reflection/fluorescence photobleaching recovery (TIR/FPR) technique (Thompson et al. 1981. *Biophys. J.* 33:435) is used to study adsorbed bovine serum albumin dynamics at a quartz glass/aqueous buffer interface. Adsorbed fluorescent labeled protein is bleached by a brief flash of the evanescent wave of a focused totally internally reflected laser beam. The rates of adsorption/desorption and surface diffusion determine the subsequent fluorescence recovery. The protein surface concentration is low enough to be proportional to the observed fluorescence and high enough to insure that the observed recovery rates arise mainly from adsorbed rather than bulk protein dynamics. The photobleaching recovery curves for rhodamine-labeled bovine serum albumin reveal both an irreversibly bound state and a multiplicity of reversibly bound states. The relative amount of reversible to irreversible adsorption increases with increasing bulk protein concentration. Since the adsorbed protein concentration appears to be too high to pack into a homogeneous surface monolayer, the wide range of desorption rates possibly results from multiple layers of protein on the surface. Comparison of the fluorescence recovery curves obtained with various focused laser beam widths suggests that some of the reversibly bound bovine serum albumin molecules can surface diffuse. Aside from their relevance to the surface chemistry of blood, these results demonstrate the feasibility of the TIR/FPR technique for measuring molecular dynamics on solid surfaces.

INTRODUCTION

Protein adsorption at a liquid/solid interface has been studied by a variety of techniques for a number of years (1–13). Interest in this subject is partially motivated by the evidence that blood coagulation on a foreign surface is mediated by a serum protein layer adsorbed from the blood onto the surface immediately after first contact. Since some surfaces are more thrombogenic than others, the details of the interaction between the surface and serum proteins appear to be of great importance in initiating thrombus formation. As both a model of this interaction and a first application of the technique of total internal reflection/fluorescence photobleaching recovery (TIR/FPR) introduced in the preceding paper (14), we examined the dynamics of fluorescence-labeled bovine serum albumin (BSA) adsorption to quartz glass. TIR/FPR measures the adsorption/desorption kinetic rate coefficients and surface diffusion coefficient of solute molecules in equilibrium with a solid surface. Knowledge of these parameters provides a detailed description of the two dimensional chemistry of serum protein/surface interaction which, in whole blood, influences the formation of a clot.

The experimental results reveal that BSA binds to quartz with a multiplicity of desorption rates which presumably reflect different classes of binding. One class is essentially irreversibly bound, and at least two other classes are reversibly bound. The ratio of reversible to irreversible binding increases with increasing bulk concentration of BSA. One interpretation is that the multiple binding classes represent multiple layers of adsorbed BSA as suggested earlier (1, 2, 4–6). TIR/FPR also suggests that BSA molecules in the most rapidly reversible class are capable of moving laterally on the surface once they are adsorbed. This surface diffusion can apparently transport adsorbed BSA molecules through a distance of at least 1 μm with a diffusion coefficient of $\sim 5 \times 10^{-9}$ cm^2/s before desorption.

MATERIALS AND METHODS

Fluorescence Excitation and Photobleaching

The purpose of the optical system (Fig. 1) is to selectively excite fluorescence-labeled adsorbed BSA in a finite area on a glass/solution surface by use of the shallow evanescent field of a totally internally reflected focused laser beam. The core of the system is a fused quartz slide (Amersil), the lower surface of which is bathed in an aqueous solution of fluorescent BSA. The laser beam (λ_0 = 514.5 nm; Lexel 95–3, Lexel Corp., Palo Alto, Calif.) passes through a spherical convex focusing lens into a cubic quartz prism which is in optical contact (via a layer of immersion oil) with the upper surface of the quartz slide.

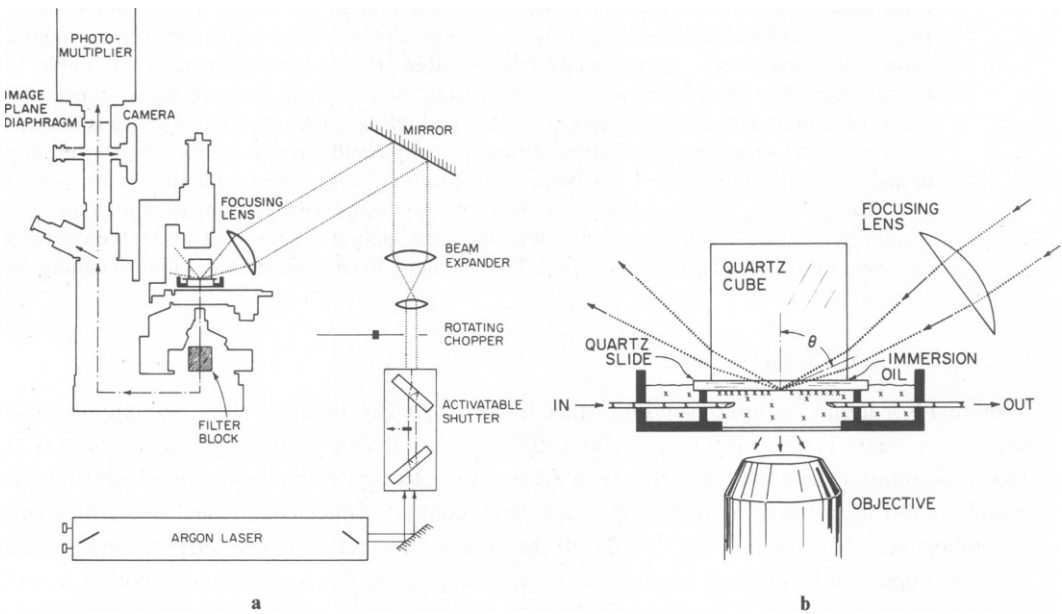

FIGURE 1 (*a*) Optical apparatus for TIR/FPR. The activatable shutter is based on the design of Koppel (16). The slowly rotating chopper wheel, which transmits the laser beam with a 20% duty cycle, is used during times long after the photobleaching flash to avoid photobleaching during extended observation. The filter block, composed of a dichroic mirror and barrier filter, is identical to one used for fluorescence microscopy by epi-illumination. (*b*) Detail of the plastic dish in which R-BSA is adsorbed to a quartz slide. R-BSA molecules are schematically indicated by ×. The median incidence angle θ = 75° for these experiments; the critical angle is θ_c = 65.4° for this system. The fused Suprasil quartz cube (Precision Cells) is 1.5 cm on a side. The hole in the bottom of the dish is covered with a glass cover slip and sealed in with encapsulating resin. The objective has a ×10 magnification and 0.25 numerical aperture.

The focal point of the beam is at the glass/solution interface, where the beam totally internally reflects. The median angle of incidence at this interface is 75°.

Fluorescence of adsorbed BSA excited by the evanescent wave is collected by the objective on an inverted microscope (Leitz Diavert, E. Leitz, Inc., Rockleigh, N.J.). In general, some nonadsorbed BSA molecules in the bulk solution within the depth of the evanescent wave (~0.1 μm) also may be excited. This contribution to the total fluorescence is usually negligible, as discussed in Appendix A. Fluorescence excited by stray light is minimized because it is out of focus and partially blocked by a diaphragm in an image plane of the microscope (part of the Leitz MPV-1 photometer). Fluorescence photons passing through this diaphragm are detected by a thermoelectrically cooled photomultiplier (RCA C31034A, RCA Electro-Optics, Lancaster, Pa.).

In TIR/FPR, as in the more conventional FPR (15), the laser beam intensity is attenuated during fluorescence observation by a shutter similar to that described by Koppel (16). A bright flash of the evanescent wave, produced when the shutter is activated, photobleaches some of the fluorescent molecules in the selectively illuminated region. A subsequent recovery of fluorescence excited by a reattenuated evanescent wave is observed as unbleached molecules replace bleached ones in the illuminated area because of adsorption/desorption and/or surface diffusion. The incident laser beam power is ~200 mW during the ~60 ms duration photobleaching flash; the power is reduced to ~1 μW during fluorescence observation.

Fluorescence intensity at the photomultiplier is monitored by a commercial photon counter system (Ortec Inc., E.G.&G., Inc., Oak Ridge, Tenn.) and converted to an analog signal. To protect the photomultiplier, its high voltage power supply is automatically modulated by a control circuit during the bright photobleaching flash. Every recovery curve in the experiments reported here was slow enough to be recorded directly onto a strip chart.

Focused Evanescent Wave Profile

The shape of the recovery curve in TIR/FPR is dependent upon the shape of the intensity profile of the evanescent wave (see companion paper, Table 1). In a homogeneous medium, the focal plane of a focused Gaussian beam retains its circular Gaussian profile (17). But in our total internal reflection system, two effects distort this profile: (*a*) refraction at the glass/air interface as the beam enters the cubic prism; and (*b*) the oblique angle formed by the optical axis of the incident beam with the glass/solution interface. A detailed derivation of the evanescent wave profile based on scalar diffraction theory has been attempted for this geometry (T. Burghardt, unpublished result). The profile critically depends upon the ratio r of the laser beam radius at the focusing lens to the focal length of that lens. In the limit of small incident beam radius ($r \sim 0.02$), calculation shows the profile to be a broad elliptical Gaussian (Table 1 of companion paper). In the opposite limit of an expanded beam at the focusing lens ($r \simeq 0.1$), the calculation shows the smaller dimension of the profile to be a narrow Gaussian. For the other dimension, the calculation is much more complicated but experimentally has been observed to be nearly constant over a length much larger than the width. Experimentally, r is adjusted by varying the beam radius at the focusing lens with a beam expander (Fig. 1 *a*). As expected from the calculation, for $r = 0.02$ we observe an elliptical profile with minor axis e^{-2} half width of 12.5 μm and an axial ratio of 2.5 (the "wide beam"); for $r = 0.1$ we observe a long thin strip with e^{-2} half width of 2.5 μm (the "narrow beam"). Actual photographs of these profiles are shown in Fig. 2.

Preparation of Tetramethylrhodamine-labeled BSA (R-BSA)

Twenty-five mg of crystallized BSA (Sigma Chemical Co., St. Louis, Mo.; essentially fatty acid free) were dissolved in 2.5 ml of pH 9, 0.1 M sodium bicarbonate buffer. An excess of tetramethylrhodamine isothiocyanate powder (Research Organics, Inc., Cleveland, Ohio) was added and allowed to react with the BSA for ~1 min with continual stirring. The reaction mixture was then passed through a column of Sephadex G-50 made in pH 7.05 mM sodium phosphate plus 150 mM NaCl buffer (PBS) to separate excess unreacted tetramethylrhodamine isothiocyanate from labeled protein. Typically, this procedure yielded 2–5 rhodamine groups/protein molecule. The labeled protein was dialyzed in distilled water for ~24 h to remove any remaining rhodamine groups that may have nonspecifically attached to the BSA.

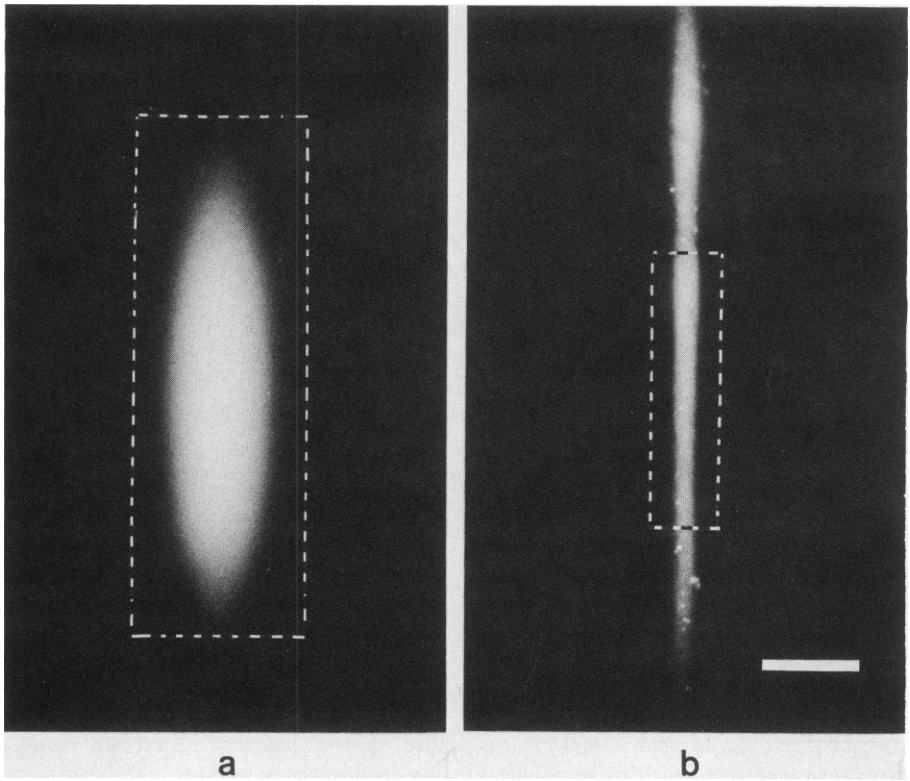

FIGURE 2 The intensity profile of the (*a*) "wide beam" and (*b*) "narrow beam." These are photographs of fluorescence excited by the evanescent wave at a quartz glass surface coated with 3,3′-dioctadecylindocarbocyanine, a positively charged fluorescent dye which strongly adsorbs to glass. Bar, 25 μm.

After lyophilization, the R-BSA was stored at 4°C until needed. For each experiment, the R-BSA was redissolved in PBS buffer.

In most experiments, the protein used was a mixture of R-BSA and unlabeled BSA. In general, R-BSA constituted 100% of the total BSA for the lowest bulk concentration experiments, and as little as 6% at the highest bulk concentration.

Surface Preparation

Before an experiment, a slide was washed with Alconox detergent (Alconox, Inc., New York), rinsed in distilled water, and submerged in chromic acid for at least 8 h. The slide was then rinsed in ethanol and stored under ethanol until needed. Just before an experiment, the slide was blown dry by a stream of pure nitrogen gas. Both new slides and previously used slides received the same cleaning process. We verified that the adsorbed R-BSA layer on used slides was thoroughly removed by this procedure by inspecting the slides under TIR fluorescence before each experiment. This surface preparation procedure follows the one outlined by Watkins (2).

Experimental Procedure

After a clean slide was mounted in the dish of the TIR/FPR apparatus, pure buffer solution containing no BSA was injected into the dish via a peristaltic pump connected to an input hypodermic needle. The optics of the system were aligned and the background fluorescence was measured. Without altering the optical alignment or the level of the solution, the buffer was withdrawn through an output hypodermic

needle by a peristaltic pump simultaneously with the injection of R-BSA solution through the input. After almost complete replacement of pure buffer solution by R-BSA solution, the pumps were shut off and the fluorescence vs. time was recorded. TIR/FPR experiments did not begin until the fluorescence had become constant, indicating that the surface layer achieved equilibrium with the bulk solution.

Calibration

It is desirable to relate the TIR fluorescence intensity detected by the photomultiplier to an actual surface concentration of adsorbed fluorophore. To perform this calibration, we measured the TIR fluorescence of a quartz slide coated with a known concentration of tetramethylrhodamine groups. This special calibration slide was prepared with 12 other identical quartz slides. These slides were positioned in series in the light beam of a spectrophotometer inside a water-tight chamber. Two of these slides served as end windows of the chamber. The chamber was filled with R-BSA solution to allow R-BSA adsorption to the slides. The slides were then washed with many rinses of pure buffer to remove all but the irreversibly adsorbed R-BSA.

The optical density D through the chamber was measured at $\lambda = 550$ nm. D is related to the surface concentration C (in molecules/cm^2) of rhodamine on each quartz slide through the relation $C = D/n\epsilon$, where ϵ is the known extinction coefficient ($\epsilon = 2.7 \times 10^{-17}$ cm^2/fluorophore group) of tetramethylrhodamine conjugated to BSA at $\lambda = 550$ nm and n ($n = 24$) is the number of quartz surfaces coated with R-BSA in the chamber. (The light absorption due to one R-BSA coated surface was too small to measure in our spectrophotometer.)

One of the chamber's end window slides (to which R-BSA was adsorbed on only one surface) was then placed in the TIR/FPR apparatus and the fluorescence intensity was measured. Any measurement of fluorescence on a sample of interest could than be converted to a surface concentration of rhodamine groups. Given knowledge of the molar ratio of rhodamine to BSA in R-BSA, we then obtained the absolute surface concentration of R-BSA.

This calibration procedure is valid only for those adsorbed fluorophore concentrations which do not appreciably perturb the evanescent field intensity. In this domain, observed fluorescence intensity is directly proportional to surface concentration. A theoretical calculation (Appendix B) considers the problem of light absorption in the surface layer and shows that, for surface concentrations used in the calibration or TIR/FPR experiments, we are always in the domain of direct proportionality between fluorescence and surface concentration.

RESULTS

Multiplicity of Adsorption/Desorption Rates

The fluorescence recovery curves for R-BSA adsorption onto quartz (e.g., Fig. 3) typically exhibit features which can be recognized qualitatively upon inspection: a fast initial recovery, a slower recovery component manifested by a long gradual upward slope, and an incompleteness such that the recovery does not reach the prebleach level within the 30–120 min duration of the experiment. To characterize the recovery curves quantitatively, we approximate each one as a sum of exponentials. (This form is suggested by the expected exponential form for TIR/FPR recoveries in the case of reaction limited kinetics and zero surface diffusion, see Eq. 44 of the companion paper.)

We express the fluorescence recovery curve $F(t)$ in a normalized form $g(t)$:

$$g(t) \equiv 1 - \frac{F(t) - F(0)}{\bar{F} - F(0)}, \tag{1}$$

where $\bar{F}$ is the equilibrium prebleach fluorescence; $F(0)$ is the fluorescence immediately after photobleaching at time $t = 0$; and $F(t)$ is the subsequent fluorescence recovery. (Note that

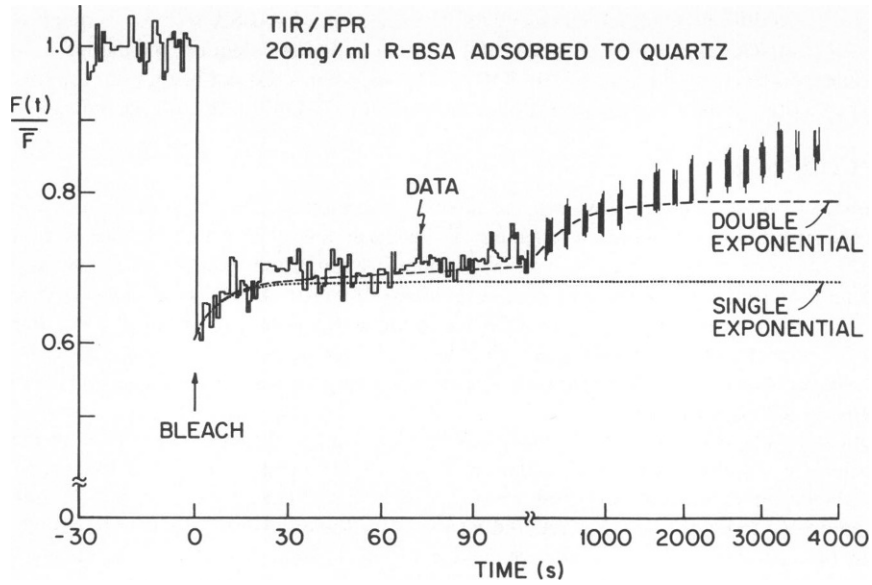

FIGURE 3 An actual TIR/FPR curve for R-BSA (20 mg/ml bulk BSA concentration) adsorption to quartz. Two types of computer-generated nonlinear least square fits are also shown. The dashed line represents the double exponential fit of the form of Eq. 2 adopted for all the analyses presented here. The dotted line represents the best single exponential fit, obtained by setting $g_1 = 0$ in Eq. 2. Although neither form fits the data well at long times, the double exponential fit is much better than the single exponential. In all such fits, a weighting function must be chosen so that later time points do not completely dominate the minimization of square deviations from the fit. The weighting function used here is proportional to the local slope of the recovery curve. This weighting forces the closest fit to occur at early times where the slope is the greatest. The fluctuations in the data are due to shot noise.

$g(t) = G(t)/G(0)$ where $G(t)$ is defined in Eq. 5 of the companion paper.) We then write $g(t)$ as a sum of exponentials:

$$g(t) = g_0 + g_1 e^{-k_2(1)t} + g_2 e^{-k_2(2)t}, \tag{2}$$

where k_2 (2) > $k_2(1)$ and $g_0 = 1 - (g_1 + g_2)$. Parameters g_1, g_2, $k_2(1)$, and $k_2(2)$ are determined by a nonlinear least squares fitting program (18) for each experimental recovery curve.

We wish to relate these fitting parameters to identifiable physical processes. We show in Appendix A that most of the fluorescence is due to R-BSA actually adsorbed to the surface rather than dissolved in bulk solution within the finite depth of the evanescent wave near the surface. We also show in Appendix C that all the recovery curves taken for bulk BSA concentrations >1 mg/ml must be reaction limited; i.e., the rate of fluorescence recovery is determined by the rates of desorption rather than the rate of diffusion of BSA molecules away from the surface in the bulk. Therefore, it is reasonable to identify the characteristic rates $k_2(1)$ and $k_2(2)$ with the desorption rates for two classes of adsorbed BSA binding: a slowly and more rapidly reversible class, respectively. (Consistent with the notation of the companion paper, we therefore use the subscript "2" for these rates to denote desorption). Factors g_1 and g_2 then represent the fraction of adsorbed R-BSA in the slowly and rapidly reversible binding

classes, respectively, and g_0 represents the fraction of R-BSA which is irreversibly bound. ("Irreversible" here is only a relative term indicating an incomplete recovery within the observation time.)

The separation of the recovery curves into components representing three parallel, noninteracting classes is the simplest model reasonably consistent with the data. A model made up of many classes of binding that interact with each other is likely more realistic. However, the noisiness and variability of the recovery curves suggests that more than the four adjustable parameters utilized in our chosen model would not add reliable information about the adsorption process.

Total Adsorption and Immobile Class g_0

The total adsorption of R-BSA to quartz (Fig. 4) increases with bulk concentration without reaching a saturation plateau in the range of bulk concentrations employed ($\leq$20 mg/ml BSA). The immobile fraction g_0, obtained by computer fit to the recovery curves, decreases with increasing bulk concentration of R-BSA. If g_0 at each bulk concentration is multiplied by the total adsorption at that bulk concentration, the absolute amount of irreversibly adsorbed

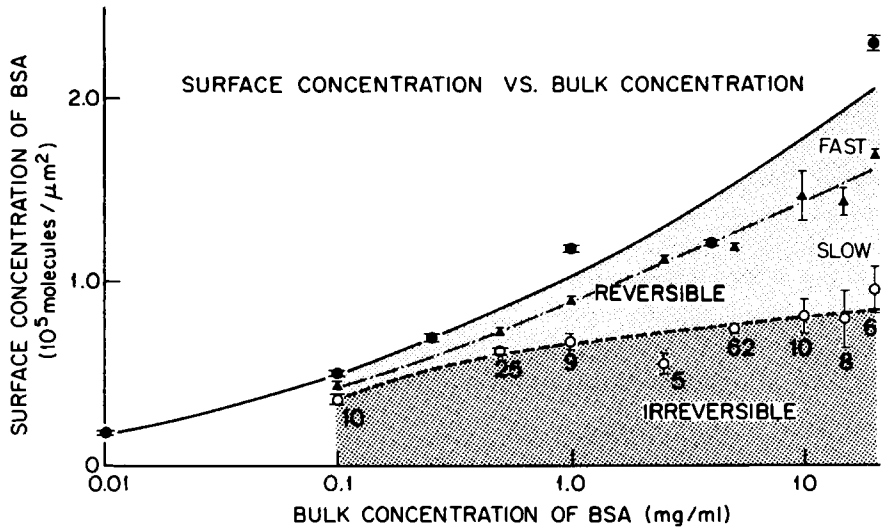

FIGURE 4 The irreversibly adsorbed BSA concentration (open circles), the sum of the irreversible and slowly reversible portions (closed triangles), and the total adsorbed BSA concentration (closed circles), as a function of bulk BSA concentration. The irreversibly adsorbed portion reaches a quasi-plateau at higher bulk concentrations whereas the total adsorption (reversible + irreversible) continues to rise. The points representing total adsorption are averages of 5–11 fluorescence readings taken at different locations on a single quartz slide, with standard error bars indicated. A smooth curve, drawn as a solid line, follows the trend of these points, but is not deliberately fit to any theoretical model. The absolute scale of the vertical axis was obtained by the calibration procedure outlined in Materials and Methods. The irreversible (----) and the irreversible plus slowly reversible (—·—) adsorption curves were obtained by multiplying the computer fitted parameters g_0 ($=1 - g_1 - g_2$) and $1 - g_2$, respectively, with the height of the total adsorption curve at the corresponding bulk concentration. The parameters are the result of averaging over many experiments on several different slides. The error bars are derived from the standard errors of g_0 and g_2 averaged over the number of runs indicated below each open bar. Absolute adsorption varied considerably ($\sim \pm 30\%$) from slide to slide, but the qualitative trends were similar on all slides.

R-BSA can be obtained (Fig. 4). Irreversibly adsorbed R-BSA increases very slowly with bulk concentrations of >1 mg/ml; the increase in total adsorption at these bulk concentrations is due almost entirely to reversible adsorption.

No significant effect of beam width on the irreversible fraction g_0 was observed. The g_0 values used for the irreversible adsorption curve of Fig. 4 were averages of all measurements of g_0 regardless of beam width.

The sorption behavior of the fluorescent proteins may be affected by the fluorophore which is covalently attached to the protein. To investigate this possibility, we varied (by a factor of two) either the rhodamine:BSA molar ratio or the labeled BSA:unlabeled BSA bulk mixture ratio (while maintaining a fixed total concentration). For each ratio, we measured the TIR fluorescence of adsorbed BSA on different slides. Preliminary results indicate that changes in the equilibrium adsorption of BSA resulting from changes in the rhodamine:BSA molar ratio or the labeled BSA:unlabeled BSA mixture ratio are less than the intrinsic variability of total adsorption from one quartz glass surface to another at fixed ratios (± 30%). Although moderate changes in the amount of rhodamine at the surface does not appear to affect a large change in adsorption, we cannot rule out the possibility that R-BSA sorption behavior is different from that of unlabeled BSA. Brynda et al. (19) have found moderate changes in adsorption of BSA after labeling by fluorescamine.

Slowly Reversible Class g_1

The fraction g_1 of slowly reversible adsorbed R-BSA increases with bulk concentration to reach a plateau around 0.30 ± 0.02 (error is SEM; the number of runs [n] is 86) at bulk concentrations $\gtrsim$3 mg/ml. There is no significant dependence of g_1 upon beam width.

The rate $k_2(1)$ for this class was highly variable from experiment to experiment, with no clear dependence upon bulk concentration. Because of this high variability, no clear dependence of $k_2(1)$ upon beam width was apparent. For bulk concentrations $\gtrsim$1 mg/ml, where the recovery is limited by reaction kinetics rather than bulk diffusion (see Appendix C), $k_2(1) = (4.6 \pm 0.9) \times 10^{-3}\ s^{-1}$ (SEM, $n = 53$) for the wide beam, and $k_2(1) = (5.0 \pm 1.0) \times 10^{-3}\ s^{-1}$ (SEM, $n = 47$) for the narrow beam.

Rapidly Reversible Class g_2 and Surface Diffusion

The fraction g_2 of rapidly reversible adsorbed R-BSA increases with bulk concentration to reach a plateau around 0.23 ± 0.01 (SEM, $n = 86$) for bulk concentrations $\gtrsim$3 mg/ml. The rate $k_2(2)$ for this class has no clear dependence on bulk concentration. However, for bulk concentrations $\gtrsim$1 mg/ml (where the recovery is limited by reaction kinetics rather than bulk diffusion, see Appendix C), $k_2(2)$ appears to depend upon beam width. Rate $k_2(2) = 0.17 \pm 0.01\ s^{-1}$ (SEM, $n = 53$) for the wide beam and $k_2(2) = 0.26 \pm 0.02\ s^{-1}$ (SEM, $n = 47$) for the narrow beam. This dependence of $k_2(2)$ on the beam width is consistent with the hypothesis that surface diffusion of R-BSA increases the recovery rate as the beam width decreases.

An approximate value for the surface diffusion coefficient D_C can be obtained by making use of the fitting program associated with Eq. 2. In a three noninteracting component model where surface diffusion affects only the most rapidly reversible component, $g(t)$ has the form (14):

$$g(t) = g_0 + g_1 e^{-k_2(1)t} + g_2 e^{-k_2(2)t}/(1 + 4\,D_C t/s^2)^{1/2}, \quad (3)$$

where s is the characteristic width of the beam. Assuming the fluorescence recovery for the wide beam intensity is independent of surface diffusion,[1] the values for $k_2(1)$ and $k_2(2)$ obtained from the computer fit of the wide beam recovery curves using Eq. 2 represent the true desorption rates for R-BSA. The values of g_1 and g_2 are found from the computer fit of curves from both beam widths, as reported earlier, using Eq. 2. Given these values of $k_1(1)$, $k_2(2)$, g_1, and g_2, we generate, from Eq. 3, simulated narrow beam $g(t)$ curves using various trial values of D_C. We analyze these simulated curves with the fitting program based on Eq. 2, adjusting D_C until the program produces a $k_2(2)$ which matches the known narrow beam experimental value (0.26 s^{-1}) as well as returns the correct experimental values of g_1, g_2, and $k_2(1)$. This particular D_C, the best estimate of the R-BSA surface diffusion coefficient, is $(5 \pm 1) \times 10^{-9}$ cm^2/s in our experiments.

We have conducted control experiments to see if the faster recovery rate observed in the narrow beam experiments could be caused by systematic artifacts arising from intense illumination. It has been suggested that illumination may (20, 21) or may not (22) cause a photochemical alteration, especially by crosslinking. Crosslinking would presumably slow fluorescence recoveries by retarding the surface diffusion and/or desorption rates of reversibly adsorbed components. In these experiments we varied the amount of photobleaching determined experimentally by the ratio of $F(0)/F(-)$, i.e., the initial fluorescence immediately after bleaching to the prebleach fluorescence, by changing the duration of the bleaching pulse and/or the intensity of the focused laser beam. Our findings, although noisy, indicate no tendency of adsorbed R-BSA fluorescence recoveries to become slower as intensity is increased over a factor of three through the range used for typical TIR/FPR experiments. Furthermore, the amount of photobleaching was very similar for both narrow and wide beam experiments, typically $F(0)/F(-) \simeq 0.7$.

DISCUSSION

Research on serum protein adsorption is motivated by its relevance to surface-triggered blood coagulation. Adsorption of plasma proteins, particularly serum albumin, is the first event in the interaction of blood with a surface. Albumin has been specifically implicated in the coagulation mechanism, since surfaces precoated with albumin appear less thrombogenic than uncoated surfaces (4, 9). Furthermore, it has been shown that albumin is preferentially adsorbed, relative to other plasma proteins, to less thrombogenic surfaces (12). These properties, as well as the high albumin concentration in the blood, stir considerable interest in the basic surface physical chemistry of serum albumin.

We have utilized a new technique combining total internal reflection fluorescence with fluorescence photobleaching recovery to examine the kinetic behavior of rhodamine-labeled BSA adsorbed to quartz glass. The most significant results are: (*a*) Adsorbed R-BSA exhibits

[1]To justify this assumption, we will demonstrate the implausibility of its opposite. Assume, then, that the rapid component of the wide beam recovery is strongly determined by surface diffusion. Since the width s_N of the narrow beam is approximately a factor of five smaller than the width s_W of the wide beam, we would expect the rapid component of the narrow beam recovery to be approximately a factor of 25 faster than that of the wide beam recovery. But a factor of only ~1.5 is observed experimentally. Therefore, the wide beam recovery is quite far from the regime in which surface diffusion is significant.

at least three desorption rates k_2: irreversible ($k_2 < 10^{-4}\ s^{-1}$); slowly reversible ($k_2 \approx 5 \times 10^{-3}\ s^{-1}$); and rapidly reversible ($k_2 \approx 0.17\ s^{-1}$). (*b*) Increasing bulk concentration increases the ratio of the reversible to irreversible adsorption. (*c*) BSA molecules in the most rapidly reversible class appear to diffuse laterally on the surface for distances $\gtrsim 1\ \mu m$ before desorption, with a diffusion constant of $\sim 5 \times 10^{-9}\ cm^2/s$.

We speculate that the various classes of adsorption represent different bound layers. The irreversible layer would form in direct contact with the glass surface. Reversible layers would next form on top of the irreversible layer with the most reversibly adsorbed layer farthest from the glass surface. This multilayer hypothesis is supported by our data which suggest that the observed surface concentration of R-BSA for bulk concentrations >0.1 mg/ml exceeds the maximum possible packing density for a monolayer of adsorbed BSA molecules which retain their native dimensions (23). The multilayer adsorption could be very heterogenous with some areas of the surface highly layered and others virtually bare, reflecting charge inhomogeneity in the quartz glass surface. The high observed surface concentration is still consistent with monolayer formation if the actual surface is very irregular on a molecular scale or if the adsorbed BSA molecules squeeze into a more compact conformation than their native bulk state.

Monolayer protein adsorption to glass has been inferred from previous work because the adsorption curve follows the Langmuir isotherm shape (1, 3). These studies report partial irreversibility in the adsorbed monolayer, which is attributed to heterogeneity in the surface binding sites. The adsorption of plasma proteins such as albumin, fibrinogen, and γ-globulin on surfaces other than glass has more recently been investigated with the same observation of reversibility in the adsorption (1, 2, 4–6). In this literature, however, reversibility is attributed to a multiplicity of bound layers.

Our results suggest the presence of surface diffusion of adsorbed BSA. This is a phenomena of considerable interest which has not been directly explored previously for any adsorbed biomolecule by any experimental technique. The possible presence of surface diffusion in the most rapidly reversible layer implies that the energy barriers to lateral motion are lower than the energy barrier to leaving the vicinity of the surface. Lateral collision based surface chemistry, a process made possible by surface diffusion, may be of importance in the mechanism of blood coagulation.

Aside from the information obtained about BSA adsorption to quartz glass, these experiments demonstrate the feasibility and utility of TIR/FPR as a technique. Using TIR/FPR, we have measured desorption rates of R-BSA and detected surface diffusion on a system in equilibrium without requiring any intrinsic spectroscopic changes between the bound and unbound states. Extension of this technique to other systems in which fluorescent ligands in bulk solution interact with surface immobilized receptors appears promising.

APPENDIX A

Dominance of Surface Fluorescence

For TIR/FPR results to characterize surface dynamics, it is essential that most of the fluorescence arises from surface adsorbed fluorophore rather than bulk dissolved fluorophore within the exponentially decaying finite depth of the evanescent intensity. The ratio R of bulk fluorescence to surface fluorescence is $\bar{A}d/\bar{C}$, where $\bar{A}$ is the bulk concentration of fluorophore, $\bar{C}$ the surface concentration, and d the e^{-1} characteristic depth of the evanescent intensity. With our angle of incidence, $d = \lambda_0/6$ (14),

where λ_0 is the excitation light wavelength in vacuum. R increases with increasing bulk concentration. For the largest bulk concentration observed here, $R = 0.071$. This implies that, at the minimum, 93% of the observed fluorescence is due to surface adsorbed fluorophore in any experiment we have reported here.

APPENDIX B

Proportionality of Fluorescence and Surface Concentration

We wish to determine the domain in which fluorescence emission is proportional to the surface concentration of an adsorbed fluorophore, with particular application to the case of R-BSA in the

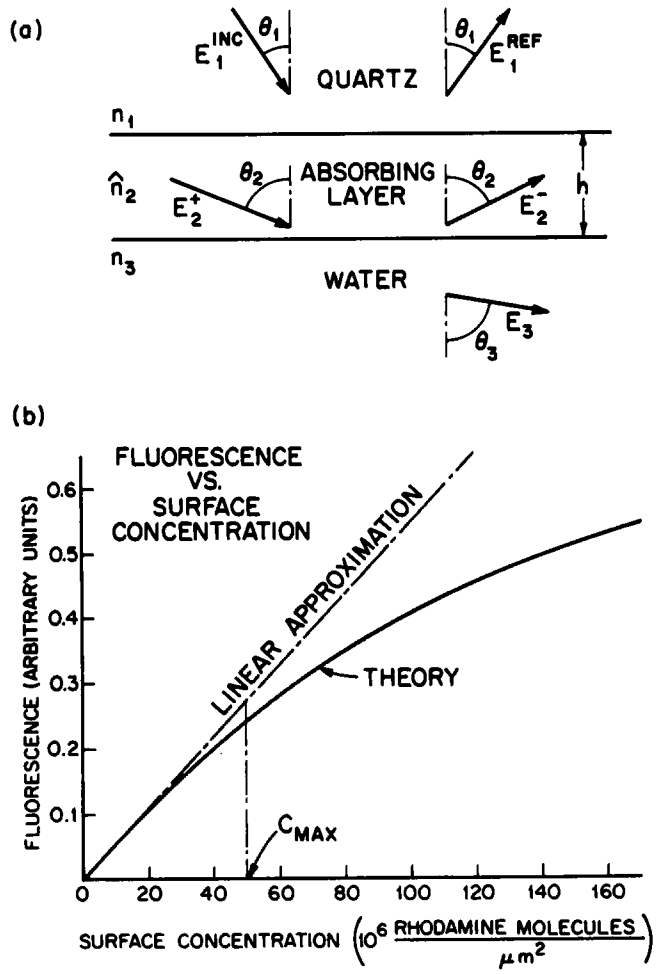

FIGURE 5 (*a*) A schematic representation of the adsorbed R-BSA layer at a quartz/solution interface. All of the electric field vectors E represent total fields inside the respective regions with refractive indices n_1, $\hat{n}_2$, and n_3. The index of refraction inside the absorbing medium is complex as signified by the symbol ^ in $\hat{n}_2$. (*b*) A plot of fluorescence versus surface concentration of tetramethylrhodamine for the system pictured in *a*. C_{MAX} is the maximum surface concentration for which the deviation of the linear approximation from the exact curve is <10%. The values for n_2 and d are not precisely known but were chosen from within reasonable ranges to give the smallest C_{MAX}. For this graph, $n_1 = 1.467$, $n_2 = 1.467$, $n_3 = 1.334$, $h = 300$ Å.

present experiments. In this domain, the evanescent field is negligibly perturbed by the adsorbed fluorophore. Since the observed fluorescence intensity is proportional to the light intensity I^{abs} absorbed by the adsorbed layer, we calculate I^{abs} as a function of surface concentration.

Consider a medium of index of refraction n_1 (quartz) separated from a medium of index of refraction n_3 (protein solution) by a light-absorbing layer of thickness d and complex index of refraction $\hat{n}_2 = n_2(1 - i\kappa)$ (see Fig. 5 *a*). Plane wave light of wavelength λ_0 is incident upon the layer from medium 1 so that total internal reflection occurs at either the first or second interface. Noting that $I^{abs} = I^{inc} - I^{ref}$, where I^{inc} is the incident intensity and I^{ref} is the reflected intensity, we write an expression (24) for the reflected electric field amplitude E_1^{ref} relative to the incident field amplitude E_1^{inc}:

$$\frac{E_1^{ref}}{E_1^{inc}} = \frac{r_1 + r_2 e^{-2i\delta}}{1 + r_1 r_2 e^{-2i\delta}}, \tag{B1}$$

where $\delta = (2\pi/\lambda_0)\,\hat{n}_2 d \cos\theta_2$; and r_1 and r_2 are the Fresnel coefficients given below:

$$r_1^{\perp} = \frac{n_1 \cos\theta_1 - \hat{n}_2 \cos\theta_2}{n_1 \cos\theta_1 + \hat{n}_2 \cos\theta_2} \qquad r_1^{\parallel} = \frac{\hat{n}_2 \cos\theta_1 - n_1 \cos\theta_2}{\hat{n}_2 \cos\theta_1 + n_1 \cos\theta_2}$$

$$r_2^{\perp} = \frac{\hat{n}_2 \cos\theta_2 - n_3 \cos\theta_3}{\hat{n}_2 \cos\theta_2 + n_3 \cos\theta_3} \qquad r_2^{\parallel} = \frac{n_3 \cos\theta_2 - \hat{n}_2 \cos\theta_3}{n_3 \cos\theta_2 + \hat{n}_2 \cos\theta_3}. \tag{B2}$$

Superscripts $\perp$ and $\parallel$ refer to electric field polarization perpendicular and parallel to the plane of incidence, respectively. Eq. B1 is valid for either polarization with the appropriate set of Fresnel coefficients. Eq. B1 is also valid without modification for reflection occurring at either interface.

Combining Eqs. B1 and B2 and calculating intensity $I^{ref} = |E_1^{ref}|^2$, we obtain I^{ref} as a function of κ. Utilizing $\kappa = \bar{C}\epsilon\lambda_0 \ell n 10/4\pi n_2 d$, I^{abs} can be plotted as a function of surface concentration $\bar{C}$. In the case of adsorbed tetramethylrhodamine (Fig. 5 *b*), the fluorescence is linearly proportional to $\bar{C}$ up to $\bar{C}_{MAX} \approx 5 \times 10^{15}$ tetramethylrhodamine groups/cm^2.

APPENDIX C

Reaction vs. Bulk Diffusion Limit

The theory of TIR/FPR (14) is simplest when the system is in the reaction limited state. In this state, when a typical bleached fluorophore desorbs from the surface, it rapidly diffuses away so that the probability of it readsorbing to the surface during the course of the experiment is essentially zero. The fluorescence recovery is then given in Table I of the companion paper for a monokinetic system.

The system can be shown to be in the reaction limit if the characteristic time for recovery in a TIR/FPR experiment is much larger than the calculated characteristic time $1/R_{BND}$ for bulk diffusion away from the surface. $1/R_{BND}$ is given by (Eq. 40 of the companion paper):

$$1/R_{BND} = \left(\frac{\bar{C}}{\bar{A}}\right)^2 / D_A, \tag{C1}$$

where D_A is the bulk diffusion coefficient; $\bar{A}$, the bulk concentration, is a known experimental variable; and $\bar{C}$, the surface concentration, is known from the calibration of the optical system. Our TIR/FPR curves for adsorption for $\bar{A} > 1$ mg/ml have recovery times at least 20 times larger than the corresponding $1/R_{BND}$ calculated from Eq. C1. This implies that for $\bar{A} > 1$ mg/ml, the recovery is in the reaction limit.

We thank Ms. Shirley Mieras and Ms. Mae Gillespie for typing the manuscript. This work was supported by a Research Corporation Cottrell Research Grant, American Chemical Society-Petroleum Research Fund grant

10590-G5,6, a University of Michigan Rackham Faculty Research Grant, and National Institutes of Health grants 1R01-NS14565 and 1R01-HL24039.

Received for publication 10 June 1980.

REFERENCES

1. BRASH, J. L., and D. J. LYMAN. 1971. Adsorption of proteins and lipids to nonbiological surfaces. *In* The Chemistry of Biosurfaces. M. Hair, editor. Marcel Dekker Inc., New York. 177.
2. WATKINS, R. W., and C. R. ROBERTSON. 1977. A total internal-reflection technique for the examination of protein adsorption. *J. Biomed. Mater. Res.* **11**:915.
3. MACRITCHIE, F. 1978. Proteins at interfaces. *Adv. Prot. Chem.* **32**:283.
4. WALTON, A. G., H. GERSHMAN, and M. E. SODERQUIST. 1977. Model biological interfaces. *Croatica Chemica Acta.* **50**:197.
5. BAGNALL, R. P., and J. A. D. ANNIS. 1978. A novel technique for studying the adsorption of plasma proteins on hydrophobic surfaces. *J. Biomed. Mater. Res.* **12**:653.
6. GENDREAU, R. M., and R. J. JAKOBSEN. 1979. Blood-surface interactions: Fourier transform infrared studies of protein surface adsorption from flowing blood plasma and serum. *J. Biomed. Mater. Res.* **13**:893.
7. KIM, S. W., and E. S. LEE. 1979. The role of adsorbed proteins in platelet adhesion onto polymer surfaces. *J. Polym. Sci. Polym. Symp.* **66**:429.
8. VROMAN, L., and A. L. ADAMS. 1971. Peculiar behavior of blood at solid interfaces. *J. Polym. Sci. Part C.* **34**:159.
9. ADDONIZIO, V. P., E. J. MACARAK, K. C. NICOLAOU, L. H. EDMUNDS, and R. W. COLMAN. 1979. Effects of prostacyclin and albumin on platelet loss during in vitro simulation of extracorporeal circulation. *Blood.* **53**:1033.
10. NEUMANN, A. W., M. A. MOSCARELLO, W. ZINGG, O. S. HUM, and S. K. CHANG. 1979. Platelet adhesion from human blood to bare and protein-coated polymer surfaces. *J. Polym. Sci. Polym. Symp.* **66**:391.
11. IHLENFELD, J. V., and S. L. COOPER. 1979. Transient in vivo protein adsorption onto polymeric biomaterials. *J. Biomed. Mater. Res.* **13**:577.
12. CHIU, T. H., E. NYILAS, and L. R. TURCOTTE. 1978. Microcalorimetric and electrophoretic studies of protein sorption from plasma. *Trans. Am. Soc. Artif. Intern. Organs.* **24**:389.
13. BRASH, J. L., and S. UNIYAL. 1979. Dependence of albumin-fibrinogen simple and competitive adsorption on surface properties of biomaterials. *J. Polym. Sci. Polym. Symp.* **66**:377.
14. THOMPSON, N. L., T. P. BURGHARDT, and D. AXELROD. 1981. Measuring surface dynamics of biomolecules by total internal reflection fluorescence with photobleaching recovery or correlation spectroscopy. *Biophys. J.* **33**:435–454.
15. AXELROD, D., D. E. KOPPEL, J. SCHLESSINGER, E. ELSON, and W. W. WEBB. 1976. Mobility measurement by analysis of fluorescence photobleaching recovery kinetics. *Biophys. J.* **16**:1055.
16. KOPPEL, D. E. 1979. Fluorescence redistribution after photobleaching. A new multipoint analysis of membrane translational dynamics. *Biophys. J.* **28**:281.
17. YOSHIDA, A., and T. ASAKURA. 1974. Electromagnetic field near the focus of gaussian beams. *Optik.* **41**:281.
18. BEVINGTON, P. R. 1969. Least squares fit of non linear parameters. *In* Data Reduction and Error Analysis for the Physical Sciences. McGraw-Hill, New York.
19. BRYNDA, E., J. DROBNIK, J. VACIK, and J. KALAL. 1978. Protein sorption on polymer surfaces measured by fluorescence labels. *J. Biomed. Mater. Res.* **12**:55.
20. SHEETZ, M. P., and D. E. KOPPEL. 1979. Membrane damage caused by irradiation of fluorescent concanavalin A. *Proc. Natl. Acad. Sci. U.S.A.* **76**:3314.
21. LEPOCK, J. R., S. D. CAMPBELL, M. GRUBER, and J. KRUUV. 1979. Photo induced cell killing and crosslinking of fluorescene conjugated concanavalin A to cell surface proteins. *Biochem. Biophys. Res. Commun.* **91**:1157.
22. JACOBSON, K., Y. HOU, and J. WOJCIESZYN. 1978. Evidence for lack of damage during photobleaching measurements of the lateral mobility of cell surface components. *Exp. Cell Res.* **116**:179.
23. PETERS, T., and R. G. REED. 1977. Serum albumin: conformation and active sites. *In* Albumin: Structure, Biosynthesis, Function. T. Peters and I. Sjöholm, editors. Pergamon Press, New York. 14.
24. HEAVENS, O. S. 1955. Thin film optics. *In* Optical Properties of Thin Solid Films. Academic Press, Inc., New York. 46.